UKAEA FUS 499

EURATOM/UKAEA Fusion

Kinetics of bubble growth and point defect migration in metals

J.H. Evans

October 2003

EURATOM/UKAEA Fusion Association

Culham Science Centre
Abingdon
Oxfordshire
OX14 3DB
United Kingdom

Telephone: +44 1235 464181
Facsimile: +44 1235 466435

Contents

Dr. J. H. Evans

jhevans@lineone.net
+44-1235-525059

Introduction

The first of the three chapters in this report covers an extension to recent work in which unusual results during the annealing of near-surface bubbles in copper were repeated in a computer simulation study. It seemed that at some threshold, breakaway swelling was occurring. In the present report, this work is extended to the simpler case of uniform helium level in the bulk, thus allowing the threshold to be studied without the complications of varying helium level and gas release at surface. The results show that under equilibrium conditions at high temperatures ($>0.35T_m$) the expected bubble coarsening with time leads, at ~20% swelling, to some breakaway effect where the swelling increases extremely rapidly This result is examined at different helium levels in copper but is also extended to other metals and helium levels. This allows a prediction of the time taken for the breakaway swelling to occur.

The results on this new topic, both for the near-surface case and for the bulk case, could be of importance in predicting the behaviour of helium in fusion power plant materials. Even small amounts of helium could cause untoward effects if materials were held at moderate temperatures for long times, or inadvertently at high temperatures for short times – as might occur under accident or loss of coolant situations.

The second and third chapters are connected by the phenomenon of void lattice formation in irradiated metals. It is generally agreed that void lattice formation reflects the long range anisotropic behaviour of self-interstitial atoms (SIAs). In cubic metals, three possibilities have been proposed: one-dimensional SIA diffusion, two-dimensional SIA diffusion, and the glide of small self-interstitial clusters formed at the periphery of collision cascades. The second chapter covers some of the difficulties in molybdenum in reconciling the theoretical and experimental studies on the properties of the self-interstitial. The third chapter examines the experimental evidence for the apparent coincidence of saturation swelling with void lattice formation and suggests this supports the two dimensional diffusion model.

For fusion power plant designers, the connection between the kinetic properties of SIAs and void swelling is potentially important. If there was agreement on our understanding of void swelling saturation, and thus on the predictions of a void swelling limit, this would give considerable confidence in the use of void lattice forming metals for fusion power plant components.

Acknowledgement

The author thanks Sergei Dudarev and Ian Cook for their interest in this work.

Chapter 1

Breakaway bubble growth during the annealing of helium bubbles in metals

1. Introduction

A recent experimental study in Delft [1] in which copper was implanted with helium ions to give a peak helium level of less than 2% at 130 nm from the surface produced the surprising result that after annealing at 973K, ~80% of the helium was released and surface pinholes seen, even though the average bubble size predicted from migration and coalescence theory was ~13nm. In modelling this situation using kinetic Monte Carlo methods to carry out computer simulations [2], an unexpected phenomenon was found in which at sufficient values of local swelling, superlarge bubbles were formed which bisected the surface, thus providing a probable explanation for the surface observations. Furthermore the density of the bubbles fitted the observed pinhole density rather well, as well as the magnitude of the gas release.

Following this work, it was felt that this phenomenon deserved further investigation in relation to its possible application to fusion environments. Although the modelling could be applied to any particular case of near surface behaviour, it appeared that further insight might be gained by investigating the fundamental rules controlling the formation of the large bubbles (probably at some critical swelling, but possibly at some other bubble concentration - radius combination). In addition it seemed useful to map out the rapid increase in swelling associated with the large bubbles. The present investigation therefore describes the simulation of gas bubble annealing in a bulk situation thus avoiding any complication due to initial non-uniform helium concentrations or to bubble loss at surfaces. The results of this investigation are presented in this chapter.

2. Outline of modelling

Brief details will be given here; a fuller description of the methodology is given in the appendix. In the main computer program an initial population of 4000 bubbles was set up in a pseudo-random distribution within a $(100\ \text{nm})^3$ block. The distribution was made following a procedure suggested by Foreman [3], with every new position being tested against all previous bubble coordinates to ensure that a minimum distance always existed between positions. The starting radius was chosen to reflect the helium level being studied. To prevent too much quantization of bubble radii after coalescence, the starting radii were treated to give a Gaussian distribution of radii about the average. In the

simulation of the high temperature anneal, the modelling simulated the random walk of bubbles, allowing the migration and coalescence of the bubbles to be followed under thermal equilibrium conditions. Spherical equilibrium bubbles were assumed, with coalesced bubbles immediately re-equilibrating to a new radius to maintain the usual $P = 2\gamma/r$ relation where P is the bubble pressure, r its radius and γ the surface energy. Since the aim of this work was to provide a qualitative picture of the bubble behaviour, the calculations were simplified by using the ideal gas law to relate the bubble sizes with their helium content.

The model allowed individual bubbles to move randomly according to surface diffusion kinetics given by the appropriate equation for bubble diffusion, D_b, [4,5]

$$D_b = (3\Omega^{4/3})/(2\pi r^4)D_s \quad (1)$$

where Ω is atomic volume of the matrix and D_s the surface diffusivity, is given by

$$D_s = D_o\exp(-E_s/kT), \quad (2)$$

where E_s is the activation energy for surface diffusion. Using random walk theory, it is easy to show that for a bubble with radius r_i, the jump-step in a given time is proportional to $1/r_i^2$. After each jump-step cycle in which all bubbles were moved, bubbles were tested against their near neighbours for touching, and if so were allowed to coalesce, to give a new bubble with a radius reflecting its new larger helium content. Because of the inverse relation of bubble pressure with radius, any coalescence under equilibrium bubble conditions leads, as is well known, to an increase in the vacancy to helium atom ratio and hence an increase in local swelling. Bubbles were also tested in position against the block surfaces. If they crossed the surface, they were introduced on the opposite face to maintain periodic boundary conditions. The overall procedure allowed the bubble size parameters and swelling to be followed with time.

One problem with modelling coalescence events is that the process leads to a reduction in bubble numbers and therefore in statistics. In a recent simulation of Ostwald ripening (for voids in silicon [6]), an analogous problem was treated by using a cloning procedure. In the present case, after the bubble numbers were reduced by a factor of eight from 4000 to 500, the block was cloned and used to create a new block with volume a factor of eight greater, thus returning to 4000 bubbles in the system but maintaining the radius distributions. While the local spatial distributions of bubbles within the eight sub-blocks were initially identical, their subsequent random movement quickly introduced differences. This iteration procedure could be repeated as many times as required.

The swelling value in the work was always defined (arbitrarily) as the bubble volume divided by the original volume. Since these values reached 20% and greater, it was felt important to reflect this swelling, and make the simulation far more realistic, by increasing the block size. At regular intervals the size of the block, and all the bubble positions, were changed appropriately, therefore maintaining the amount of material in the block. In the results to follow, all the calculations were made using nominal parameters for copper at 973K. The most important parameter was the surface diffusivity in which the expression of Escobar Galindo et al. [1] was used, i.e.

$$D_s = 1.08\ 10^{-3} \exp(-1.0eV/kT)\ \mathrm{cm}^2/\mathrm{s},$$

based on a calculated pre-exponential (= $10^{13}\lambda^2/6\ \mathrm{cm}^2/\mathrm{s}$, where λ is the jumpstep) and an activation energy of approximately half the self-diffusion energy.

3. Results

The work to date has concentrated on studying the evolution of bubbles in copper at 973K. As discussed later there was no difficulty in principle in extrapolating the results to other temperatures. Three different helium concentrations – 1, 2, and 3 at% - were studied. The main qualitative result in all cases was exactly as found in the simulation of results for implanted helium.

3.1 Breakaway bubble formation

During the first part of the anneals, the bubble coarsening behaviour was much as expected, with a gradual coarsening of the bubble populations with the average radius closely following the expected $t^{(1/5)}$ variation with time [7,8]. In this region all runs gave results which were quantitatively extremely close. However, eventually, out of what appeared to be a typical cluster of bubbles, a large bubble was formed. Although, as shown later, there were clear variations between computer runs for the annealing time required to form these large bubbles, the qualitative picture was always the same. An example of the evolution during the formation of the large bubble is given in Fig.1.

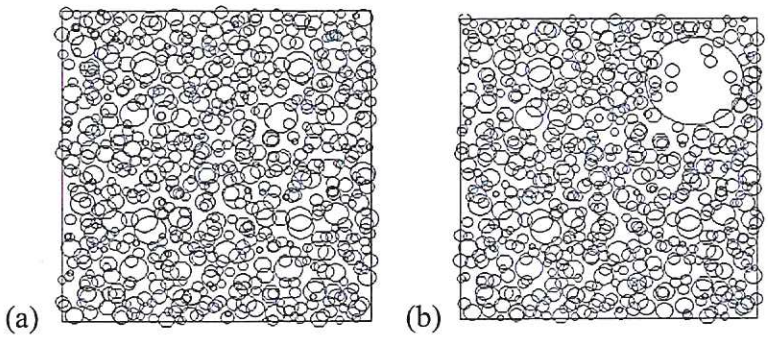

Fig.1 Section through the bubble volume showing the rapid formation of a large bubble; (a) time = 34.6s, (b) time = 41.3s. The projected area has sides of 424 nm.

The formation of the large bubbles was reflected in the bubble and swelling parameters, and is seen in Fig.2 in an example from a computer run for 2 at% helium. The smooth rise in all these parameters is interrupted by the sudden rises in the swelling and in the value of the root mean cube radius.

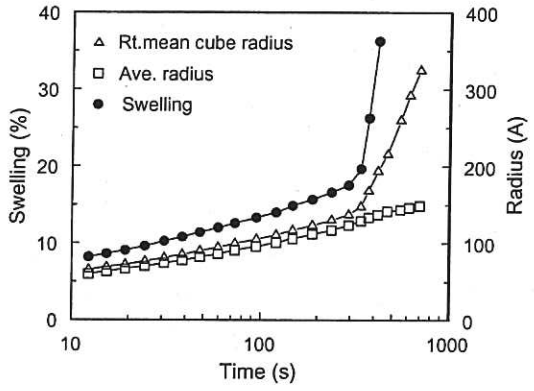

Fig.2. Typical results, here for 2 at% He, showing the sharp break-away in the swelling and root mean cube radius coincident with the formation of large bubbles

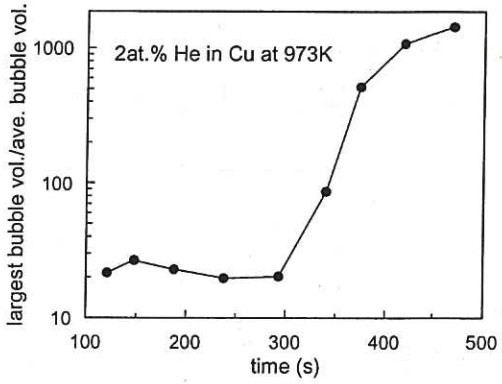

Fig.3. Graph showing the rise in ratio of largest bubble volume to the average bubble volume as a function of time

A third way of demonstrating the breakaway effect is in a plot of the volume of the largest bubble, easily extracted from the data, compared to the value of the average bubble. As shown in Fig.3, this ratio changes over a relatively short period from a steady state value (of between 10 and 20) to a value well in excess of 1000.

3.2 Statistics

Since the bubble movements are random, it was important to get a feel for the repeatability of the results. As already mentioned, up to the breakaway point, the bubble parameters were very consistent from run to run. However, the breakaway point varied considerably. This is demonstrated for the 3% helium case in Fig.4.

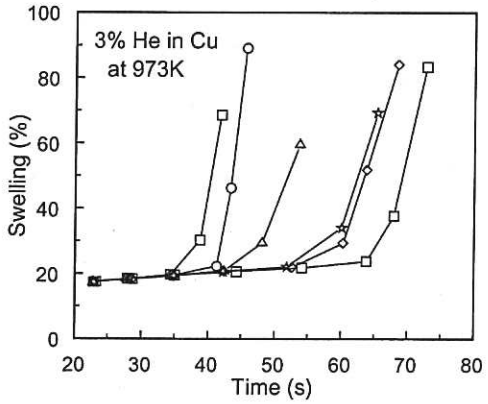

Fig.4 Bubble swelling as a function of time for 3%He in copper at 973K showing the run to run variations for the breakaway swelling.

The variation seen here, between about 35 and 65 minutes was surprisingly large, but the same order of variation was also found for the 1 and 2% helium levels.

3.3 Influence of helium content

As expected, the helium level was found as expected to have a marked effect on the time required for the breakaway swelling to occur. This is seen in Fig.5 where representative data for three helium levels are shown. It became clear that the large bubbles formed when the average swelling reached approximately 20%.

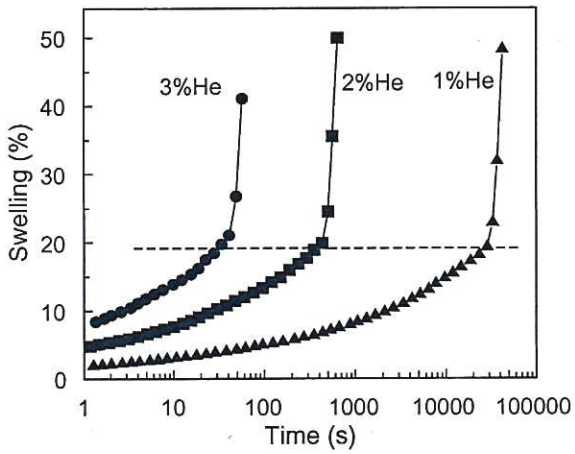

Fig.5 Effect of helium level on time to breakaway swelling. The horizontal dashed line emphasises the 20% swelling level.

As shown in the last section, the variation between computer runs meant that only a rough range could be deduced for the breakaway time. The approximate average times for this breakaway at 973K were 3 10^4 secs, 400s and 50s for 1%, 2%, and 3%He respectively.

3.4 Extrapolation to other temperatures

In the appendix it is shown that the time increments for a given set of starting conditions (i.e. given helium content) are proportional to $[(9\Omega^{4/3}/\pi)D_s]^{-1}$; the same must hold for the total sum of the increments, i.e. the total time. Thus using Eq.(1) for D_s we can write the breakaway time, t_b , as

$$t_b = K(\text{x}\%)\ \exp(+E_s/kT), \qquad (3)$$

where K(x%) is a constant for a given helium content.

The data at 973K for copper can thus be translated to any temperature provided the assumptions in the model still hold. The main problem at lower temperatures will be the slower growth of coalesced bubbles back to equilibrium. Nevertheless, if this is ignored then the K values are trivially obtained from the breakaway times already given and are: $K(1\%) = 0.194$; $K(2\%) = 2.56\ 10^{-3}$: $K(3\%) = 3.23\ 10^{-4}$. With these values it is easy to draw a graph,

below, for the breakaway time for different helium contents as a function of anneal temperature, Fig.6.

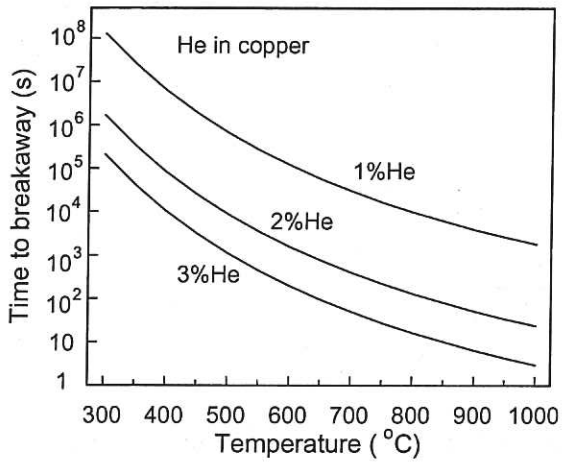

Fig.6 The extrapolation of the computed results for helium in copper at 973K to other temperatures.

3.5 Extrapolation to other metals

The key to this extension of the model is to obtain an expression for the surface diffusivity that might be applicable, in the sense of giving a guideline, to other metals. For copper, it was assumed that the activation energy for surface diffusion was half the self-diffusion energy. It is not difficult or novel to suggest a relation between activation energies and melting temperature. In Fig.7 this is done for the self-diffusion energy using data from Siegel [9].

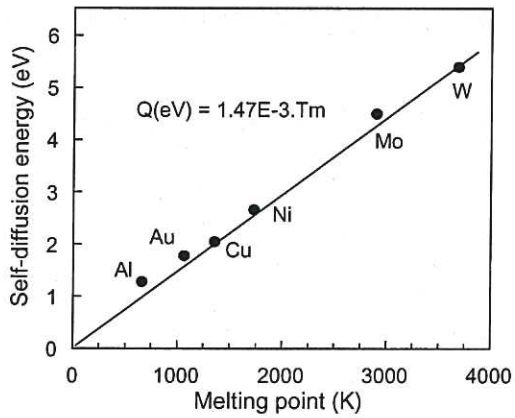

Fig.7. Self-diffusion energies for different metals as a function of melting temperature, T_m [9]

It can be seen that the relation $Q = 1.47\ 10^{-3}.T_m$ eV is a reasonable fit to the Fig.7 data. If, as for copper, the value of E_s is given by $E_s = Q/2$, then $E_s = 7.375\ 10^{-4}.T_m$. If this replaces the value of E_s in Eq.(3) then we get:

$$t_b = K(x\%) \exp (7.375\ 10^{-4}\ T_m / kT), \qquad (4)$$

This expression allow us to use the values of K obtained from copper to plot a universal curve, Fig.8, for different metals showing the breakaway time as a function of T/T_m.

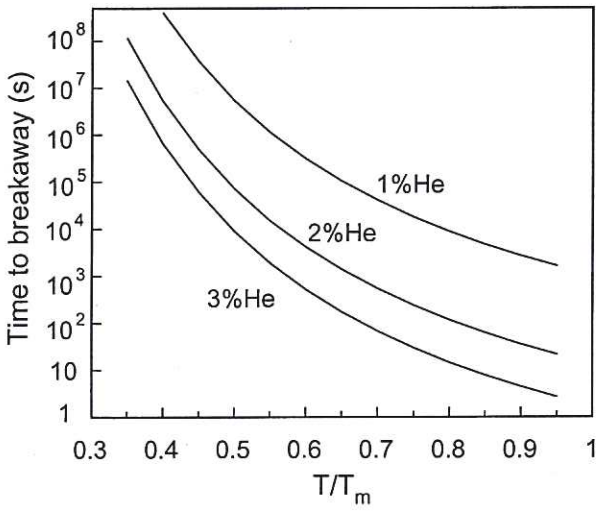

Fig.8. Universal plot of time to breakaway as a function of T/T_m, see text.

It is suggested that Fig.8 might be a reasonable guide to the importance of the breakaway swelling in practice. As modelled in this paper, the results would apply to situations where materials containing helium are then subjected to high temperature annealing.

4. Discussion

This chapter of the report has extended recent work on breakaway swelling during the annealing of near surface helium bubbles to the case of bubble swelling in bulk material, under initial conditions of a uniform helium level. Again during the computer simulation of bubble movement, and the consequent bubble coalescence, a breakaway swelling effect is seen. The effect is initiated when the average swelling reaches ~20% after which the overall swelling increases sharply to high levels.

Although any results in practice will be modified by the assumptions in the model, the qualitative effects will remain. This could be particularly important in predicting the behaviour of helium in materials under fusion power plant conditions. The results of Fig.8 would suggest that material with even low helium levels could give very high swelling values if held at moderate temperatures for long times or inadvertently (e.g. under accident conditions) at high temperatures for short times.

References

1. R. Escobar Galindo, A. van Veen, J.H. Evans, H. Schut, J. Th. M. de Hosson, Surface phenomena studies on thermally annealed helium implanted copper, May 2003, submitted to Nucl. Instr. and Methods, B.

2. J.H. Evans, R. Escobar Galindo, A. van Veen, A description of bubble growth and gas release during thermal annealing of helium implanted copper, June 2003, submitted to Nucl. Instr. and Methods, B.

3. A.J.E. Foreman, unpublished work

4. R. Kelly, Phys. Stat. Solidi 21 (1967) 451.

5. F.A. Nichols, Kinetics of diffusional motion of pores in solids, J. Nucl. Mater. 30 (1969) 143.

6. J.H. Evans, Mechanisms of void coarsening in helium implanted silicon, Nucl. Instr. and Methods B 196 (2002) 125.

7. E.E. Gruber, Calculated size distributions for gas bubble migration and coalescence in solids, J. Appl. Phys. 38 (1967) 243.

8. P.J. Goodhew, S.K. Tyler, Helium behaviour in bcc metals below $0.65T_m$, Proc. Roy. Soc. A377 (1981) 151.

9. R.W. Siegel, Atomic defects and diffusion in metals, Int. Conf. on 'Point defects and defect interactions in metals' Yamada 1981 (eds. J. Takamura, M. Doyama and M. Kiritani) Univ. of Toyko Press 1983, p.533.

Appendix

In this section we give a more formal description of the methodology used in the simulation program. In each cycle the bubbles (having a wide distribution of radii) perform one jump in a random direction, at which stage each bubble is tested against its nearest neighbours for touching, and thus whether coalescence should take place. The main question is how one chooses a time-step appropriate to the scale of the bubble distribution and diffusion parameters.

It is worth starting by introducing the main diffusion equation for bubbles, radii r, moving under surface diffusion conditions

$$D_b(r) = (3/2\pi)\,(\Omega^{4/3}/\,r^4)D_s \qquad \text{(A1)}$$

where Ω is the atomic volume of the metal and D_s is the surface diffusion coefficient.

If the jump-step cycle takes place in a time dt then the distance l moved in this time by a bubble of radius r will be

$$l(r) = \sqrt{(6D_b.dt\,)} \qquad \text{(A2)}$$

Combining Eqns. (A1) and (A2) we obtain

$$l(r) = [((9/\pi)\,\Omega^{4/3}\,D_s\,dt)^{1/2}\,]\,/\,r^2 \qquad \text{(A3)}$$

or

$$l(r) = jsp\,/\,r^2 \qquad \text{(A4)}$$

where jsp is a jump-step parameter given by $jsp = [((9/\pi)\,\Omega^{4/3}\,D_s dt)^{1/2}\,]$.

While this is useful, it is necessary to connect the scale of the bubble system to the time step. A measure of the system scale, *ss*, was chosen to be related to the bubble density, *rho*, and the average radius, r_{ave}, by the relation

$$ss = (rho)^{-1/3} - 2.r_{ave} \qquad \text{(A5)}$$

It can be seen that this is roughly the average distance between bubble surfaces. Reference has been made to the nearest neighbours of the bubbles in testing for touching. Each bubble in fact had a neighbourhood list giving the bubbles which lay within a distance *ss*; this list was revised every 100 cycles. The purpose of the list was of course to avoid the considerable computing time required if every bubble was to be tested for touching against every other bubble in each cycle. It was decided that the time step could be defined to ensure that the smallest bubble in the system (i.e. the fastest moving) should not diffuse more than the value of *ss* in the 100 cycles between the neighbourhood list revision. This in turn ensured that only the bubbles on the neighbourhood list of a given bubble could reach the bubble in the 100 jumps; thus potential collisions between bubbles would not be missed.

Random walk theory shows that in a given number of cycles, *N*, only a very small fraction of random walkers travel further than 3 times the RMS value, i.e. $3j\sqrt{N}$, where *j* is the jumpstep. If this distance is reasonably described as the maximum distance moved, then for the smallest bubble, radius r_{sml}, we can equate its maximum movement, j_{sml}, in 100 cycles to the value of the average bubble spacing, *bs*. Thus

$$bs = 3\, j_{sml}.10, \text{ i.e. } bs = 30\, j_{sml} \qquad \text{(A6)}$$

From Eq.(A4) we have $j_{sml} = jsp/r_{sml}^2$ and hence we can write

$$jsp = r_{sml}^2\, bs/30 \qquad \text{(A7)}$$

Since we already have an expression for *jsp* in terms of *dt* it is easy to rearrange the equations to obtain the relation

$$dt = jsp^2/((9/\pi)\, \Omega^{4/3}\, D_s) \qquad \text{(A8)}$$

Clearly from Eqs (A7) and (A8) the value of *dt* can be computed continuously throughout the program in terms of r_{sml} and *bs*, thus reflecting the scale of the bubble distribution and the fastest moving bubble. Results using these equations were compared with data obtained with a value of 60 instead of 30 in Eq. (A7), giving time increments a factor of 4 smaller. No differences were perceived in the data. However, after the formation of the breakaway bubbles, their growth was always faster with the larger value.

Chapter 2

The configuration and migration of self-interstitial atoms in molybdenum: a brief experimental summary

1. Background

The study of self interstitial atoms (SIAs) in metals has a long history. As emphasised in a recent paper by Han et al. [1] on SIAs in vanadium and molybdenum, they are of prime importance in high energy radiation environments and in ion implantation, particularly in respect to displacement damage effects in solids. In spite of extensive work, uncertainties with regard to the SIA structure and migration modes are still present. In particular for molybdenum and tungsten it has long been widely accepted that the stable structure from both experiment and calculations is the <011> dumbbell. Nevertheless, calculations of the structure have sometimes challenged this view; e.g. Guinan et al. [2] concluded that in tungsten the <111> crowdion was the most likely configuration. A similar conclusion to strongly challenge the conventional view comes out of the work of Han et al. [1].

A full in-depth study of this area would require considerable time and both experimental and theoretical expertise. The present short study will touch on some of the experimental work in molybdenum and also touch on the suggested role of the SIA in models of void and bubble lattice formation in molybdenum and other metals.

2. Experimental

2.1 Recovery stage for long range SIA migration

In early work the main technique used to study defect migration was that of resistivity recovery in samples irradiated at low temperature. In both fcc and bcc metals this method showed that recovery was rather more complex than expected with the appearance of several substages. In molybdenum, there appear to be two main self-interstitial recovery stages, one at ~25K and one at ~40K. Difficulties in the analysis can be seen by reference to the papers of Afman [3,4]. However, internal friction studies aimed at the detection of long range migration provided considerable help. Afman quotes the results of the Grenoble group [5,6] and in particular the attribution by this group of the internal friction peak at 40K to the free migration of interstitials. Although Afman himself was less certain of this attribution, there has been plenty of support for this in subsequent work. For example, Tanimoto et al. [7] in introducing their work on the free migration of SIAs in Mo refers to the work of Kugler et al. [8] and of

Mansel et al. [9]. The latter is interesting since it used Mössbauer spectroscopy to follow the trapping of self-interstitials at ^{57}Co impurities during the isochronal annealing of molybdenum previously electron irradiated at 4.6K, thus detecting the long range migration of self-interstitials with more certainty. The conclusion was that interstitials in Mo become mobile around 35K. (The few degrees difference between the 40K quoted earlier is of no consequence since heating rates and the number of jumps before the detection of the SIA is both concentration and technique dependent.)

The simple picture above has been complicated by the careful work of Tanimoto et al. [7] already quoted, where dislocation pinning has been used to examine the recovery stage as a function of interstitial concentration over the range 0.006 to 1.4 ppm. Tanimoto et al. suggest that the 40K peak is composed of two closely spaced constituents described as the lower temperature peak (LTP) and the higher temperature peak (HTP), the former peak dominating at low concentrations. The authors' interpretation is that the LTP and HTP reflect the migration of SIA-I and SIA-II defects.

2.2 Migration energy

The present work was partly triggered by the suggestion in Han et al. [1] that their calculated <111> dumbbell migration energy in molybdenum was zero ± 0.05eV, in agreement with experimental measurements where they quote the value of 0.05eV from the review of Young [10]. However, Young gives no value for molybdenum. Possibly Han et al. have quoted the value of 0.054 eV Young gives for tungsten from the work of Dausinger and Schultz [11]. This was for recovery between 24 and 30K. For a higher recovery temperature, as in molybdenum, a rather higher activation energy would seem appropriate. In fact, very careful resistivity measurements on molybdenum electron irradiated at 4.2K by Afman [3] showed the resistivity peak (the so-called I_E peak) at ~40K had an activation energy of 0.113 ± 004 eV, reduced to 0.107 ± 0.003 eV after background corrections.

Other work also gives energies around 0.1eV. Tanimoto et al. [7] deduce energies of 0.100 and 0.083eV for the LTP and HTP interstitial stages mentioned earlier. Thus the activation energy obtained theoretically for SIA migration appears to be too low to fit the experimental data on molybdenum.

2.3 SIA Configuration

There is no doubt that the <011> dumbbell has been widely accepted as the SIA configuration in Mo and other bcc metals. As stated by Wolf [12], referring to the review of Dederichs [13], this structure has been verified both theoretically and experimentally.

Theoretically this was still the case in 1984 when Harder and Bacon examined defect properties in bcc metals with N-body interatomic potentials [14]. However, they confirmed work by Thetford [15] in which he had found a slightly 'bent' <011> configuration when starting the relaxation procedure from an asymmetric position. This is also described by Ackland and Thetford using an improved N-body semi-empirical model [16]. Thus we have another example where the simple position has become more complicated. This has been accentuated even further by the recent work of Han et al. [1] already referred to. Reporting on an extensive ab initio study of SIA in V and Mo, they find the most stable structure to be the <111> dumbbell. However, this is qualified by the possibility that the dumbbell orientation could lie between <111> and <011> since in Mo the E_f versus dumbbell orientation is very shallow near the <111> orientation. They suggest that there could be substantial thermal wobble even at low temperatures: the resulting diffraction pattern could be compatible with the experimental data of Ehrhart [17], previously attributed to the <011> dumbbell.

The effect of temperature is important since whatever the most stable structure or jump-step at 0K, in practice we are interested in jump-steps in the 0.3 to 0.5 T/T_m where T_m is the metal's melting temperature. It is interesting that during their Mössbauer study on irradiated Mo, Mansel et al. [9] found changes in the ^{57}Co impurity-interstitial configuration during annealing.

2.4 Migration mechanisms

Tanimoto et al. [7] in examining this topic in 1994 reported that although there was agreement on the migration temperature of SIAs, the actual migration mechanism was still disputed. At this stage it was still accepted that the SIA configuration was the <011> dumbbell but as seen in the last section, the situation has become more complicated. However, even earlier Guinen et al. [2], while accepting the conventional configuration, gave results from fully dynamic computer simulation suggesting that the <011> dumbbell in tungsten migrated along the <111> direction. Less surprisingly this diffusion mode also comes out of the work of Han et al. [1] with the <111> dumbbell already mentioned.

The question for the observer is at what stage can the latest theoretical approach be frozen? With regard to the results of Han et al. a problem with the migration energy has already been indicated. For the moment this justifies the view that other possibilities should still be considered. Among these are the earlier <011> dumbbell configuration and the experimental observations by Jacques and Robrock [18] from anelastic after effect measurements in Mo that there is no reorientation of the <011> dumbbell at least up to 500K. Thus this configuration

does not undergo three dimensional diffusion. Instead they suggested that the SIA diffused via two dimensional motion, i.e. diffusion without rotation.

Other workers have also discussed this migration mode. It was first mentioned by Kronmüller as early as 1970 [19] but it is of interest that Schultz in a short review of the SIA recovery stage[20] uses planar migration to explain features of the substages in molybdenum. (Planar migration leads to differences with in-plane and out of plane recombination). Lucasson et al [21] used the dynamical properties of the dumbbell to examine the different linear relationships for fcc and bcc metals between the Debye temperature and the temperature of SIA migration. They drew attention to the fact that the bcc lattice can be deduced from the fcc by a simple geometrical transformation in which the [100] direction is crushed, one side of the cube being reduced by a factor of $\sqrt{2}$. As a result the libration mode is unique in the (011) plane instead of double in the two orthogonal (100) planes in the fcc crystal. This results in a higher efficiency of the transverse phonons in awakening the librations and promoting the jump of the defect, thus explaining the different linear relationships mentioned above. They conclude that this argument supports readily the easiest migration mechanism in bcc metals as being planar. The work of Ram [22] should also be mentioned; he looked at the dynamics of SIA in bcc metals using the Green's function method. He concluded that a two-dimensional jump through the combined effect of translation and libration provides a consistent picture of the long range migration of SIAs in molybdenum.

3. Implications of SIAs in cavity lattice formation.

Foreman [23] was the first to suggest that the SIA, by moving one-dimensionally, might provide an explanation for the formation of void lattices. This idea of anisotropic interstitial diffusion was extended by Evans [24] who used the experimental molybdenum results of Jacques and Robrock [18] above to suggest that the two-dimensional jump-step could provide an alternative explanation for void and bubble lattices. This has found support [25] in explaining the planar ordering of voids and bubbles found in hcp metals. In the cubic metals, the position has been complicated by the addition of the idea that the formation and glide (along close packed directions) of small interstitial loops formed on the periphery of collision cascades could play the crucial role [26]. Although this reference recognises the real difficulty presented by the experimental observation that void lattice formation has been found under 1 MeV electron irradiation [27] (where no cascades are formed), this evidence against the model has not prevented its further discussion in the literature [28]. On the other hand the possibility

that single interstitials migrate one dimensionally at lattice formation temperatures is still an open question.

4. Conclusions

It is hoped this chapter of the report contains some useful pointers and references to a complex area of work. Certainly several questions have been raised. Can one believe, as claimed in the careful work of Tanimoto et al. [7], that two types of interstitial coexist? How does one judge the importance of the disagreement between the very low migration energy calculated for an SIA by Han et al. [1] against the experimental value at least a factor of two larger? How does temperature influence the jump-steps calculated at zero Kelvin? Finally, with regard to void lattice formation, is there enough information from studies of the SIA behaviour (albeit in a different temperature regime) to judge the merits between one- and two-dimensional interstitial jump-step models? As an attempt to answer this last question, one could argue that a study of the void swelling (and its saturation) in the presence of void lattice formation might be useful. This will be discussed in the next chapter.

References

1. S. Han, L.A. Zepeda-Ruiz, G.J. Ackland, R. Car and D.J. Srolovitz, Self-interstitials in V and Mo, Phys.Rev.B 66 (2002) 220101(R).

2. M.W. Guinan, R.N. Stuart and R.J. Borg, Fully dynamic computer simulation of self-interstitial diffusion in tungsten, Phys. Rev.B 15 (1977) 699.

3. H.B. Afman, A method for the determination of the activation energy of recovery processes as applied to electron irradiated molybdenum, Phys. Stat. Solidi (a) 4 (1971) 421.

4. H.B. Afman, Stage I recovery of Mo irradiated at 4.2K with electron of different energies, Phys. Stat. Solidi (a) 11 (1972) 705.

5. R. Pichon, P. Bichon and P. Moser, J. Physique, Suppl.32 (1971) C2.

6. V. Hivert et al. J. Phys. Chem. Solids 31 (1969) 1843.

7. H. Tanimoto, H. Mizubayashi, N. Teramae and S. Okuda, Migration mechanism of self-interstitial atoms in Mo after low temperature irradiation I & II J. Alloys & Compounds, 211/212 (1994) 154 & 546.

8. H. Kluger, I.A. Schwirtlich, S. Takaki, U. Ziebart and H. Schultz, Int. Conf. on Point defects and defect interactions in metals, Univ. of Tokyo Press 1982, p.191.

9. W. Mansel, J. Marengos and D. Wahl, Radiation damage studies in bcc metals by Mossbauer spectroscopy, J. Nucl. Mater. 108/109 (1982) 137.

10. F.W. Young, Interstitial mobility and interactions, J. Nucl. Mater. 69/70 (1978) 310.

11. F. Dausinger and H. Schultz, Long range migration of self-interstitial atoms in tungsten, Phys. Rev. Letters 35 (1975) 1773.

12. D. Wolf, Correlation effects for interstitial-type self-diffusion mechanisms in bcc and fcc crystals, Phil. Mag. A 47 (1983) 147.

13. P.H. Dederichs, C. Lehmann, H.R. Schober, A. Scholz and R. Zeller, Lattice theory of point defects, J. Nucl. Mater. 69/70 (1978) 176.

14. J.M. Harder and D.J. Bacon, Point defect and stacking fault properties in bcc metals with n-body potentials, Phil. Mag. 54 (1986) 651.

15. R. Thetford, Harwell Report 1985, AERE M-3507.

16. G.J. Ackland and R. Thetford, An improved N-body semi-empirical model for body-centred cubic transition metals, Phil. Mag. A 56 (1987) 15.

17. P. Ehrhart, The configuration of atomic defects as determined from scattering studies, J. Nucl. Mater. 69/70 (1978) 200.

18. H. Jacques and K.-H. Robrock, Elastic after-effect studies of molybdenum after electron irradiation at 4.7K, J. de Physique, Colloque C5, supplement au N° 10, 42 (1981) C5-723.

19. H. Kronmüller, Studies of point defects in metals by means of mechanical and magnetic relaxation, Proc. Int. Conf. on Vacancies and Interstitials in Metals, Julich, 1968, (eds. A. Seeger et al.) North-Holland 1970, p.667.

20. H. Schultz, Stage II recovery reactions in bcc transition metals, Mat. Sci. Forum 15-18 (1987) 727.

21. P. Lucasson, F. Maurey and A. Lucasson, On the migration of interstitial defects in irradiated cubic metals, Mat. Sci. Forum 15-18 (1987) 231.

22. P.N. Ram, Dynamics of self interstitial atoms in bcc metals, Phys. Rev. B 43 (1991) 6977.

23. A.J.E. Foreman, A mechanism for the formation of a regular void array in an irradiated metal, Harwell Report 1972, AERE R-7135.

24. J.H. Evans, Void and bubble lattice formation in molybdenum: a mechanism based on two dimensional self-interstitial diffusion, J. Nucl. Mater. 119 (1983) 180. Also: Cavity lattice formation in metals: an experimental survey and a possible explanation based on planar diffusion of self-interstitials, Proc. Int. Meeting on Non-linear Phenomena in Materials Science, Aussois, France, Diffusion and Defect Data B, Solid State Phenom. 3/4 (1988) 303.

25. Th. Klemm and W. Frank, Void ordering in hexagonal close-packed metals, Appl. Phys, A 63, (1996) 19.

26. S.I. Golubov, B.N. Singh and H. Trinkaus, Defect accumulation in fcc and bcc metals and alloys under cascade conditions, J. Nucl. Mater. 276 (2000) 78.

27. S.B. Fisher and K.R. Williams, Void spatial regularity in an electron-irradiated stainless steel, Rad, effects, 32 (1977) 123.

28. H. Heinisch and B.N. Singh, The effects of one-dimensional mifration of self interestital clusters on the formation of void lattices, J. Nucl. Mater. 307-311 (2002) 876.

Chapter 3

A survey of experimental evidence associating saturation swelling with void lattice formation.

1. Background

The formation and growth of voids in metals subjected to displacement damage from high energy neutrons or ions has been studied for over three decades. The area has inspired a considerable theoretical effort to fully understand the underlying processes. One experimental aspect which still has no agreed explanation is the void lattice phenomenon in which voids in bcc, fcc and hcp metals are often found to be spatially ordered in structures which reflect the crystallography of the host metal, i.e. bcc in bcc metals, fcc in fcc metals, and ordering parallel to the basal plane in hcp metals. The phenomenon is a clear example of self-organisation pattern formation.

One of the first mechanisms to explain the formation in metals was that of Bullough and co-workers [1] who proposed an explanation based on elastic interaction effects. One prediction of this model was that there was an energy minimum when the ratio of void lattice parameter, A, to void radius, r, fell to a value of around 10. This raised the question of whether void growth might then stop, leading to a saturation of the void swelling value, and aroused interest in the range of A/r parameters found in experimental observations. Krishan [2], and Kulcinski et al. [3], have provided useful compilations of experimental values for A/r, though in both compilations there is occasional confusion between the void lattice parameter and the nearest neighbour distance in the void lattice. The idea of an association between saturation swelling and void lattice formation was strongly encouraged by the experimental results of Loomis et al. [4] and of Kulcinski et al. [5] and led to its general acceptance.

This association became an important part of the void lattice model based on the idea of two-dimensional self-interstitial diffusion [6]. The analysis of Evans and Foreman [7] showed that for this model the void swelling saturation was an inevitable outcome. This saturation has also been in the minds of those proposing the production bias theory of void swelling and tentatively extending it to explain void lattice formation. However, the suggestion from this work is that there is a saturation in void radius [8,9] rather than in the swelling value itself.

The question of saturation swelling is clearly of interest in relation to void lattice formation and could be an important pointer to the mechanism. The recent review of Ghoniem et al. [10] on nanostructure self-organisation in irradiated materials, together with other recent papers [9,11], has renewed interest in void lattice formation, particularly its formation mechanism. As the references in this chapter show, this has been a long standing debate. It therefore seems an opportune moment to examine the experimental work in the literature where the association of a swelling saturation with void lattice formation is discussed or can be inferred. This survey is given below.

2. Experimental survey

2.1 Bcc metals.

2.1.1 Molybdenum

The strong correlation between void lattice formation and saturation swelling in molybdenum was pointed out by Stubbins et al. [12] in discussing their extensive void results obtained during an ion implantation study. Data was obtained over a wide range of irradiation temperatures from 900 up to 1500°C. They found both void lattice formation and low swelling (<3%) at sample temperatures below 1100°C ($0.47T_m$) but above 1200°C, where no lattice formation was observed, swelling values varied from ~6 to ~12%. From these results Stubbins et al. concluded that void ordering controls the swelling in molybdenum up to 1100°C but that above this temperature voids can grow uninhibited by the restriction of void lattice formation. In addition they emphasised the 3% swelling value found in the void lattice formation temperature range.

More support for a saturation of swelling in molybdenum comes from the work of Garner and Stubbins [13] who examined this particular point with regard to both their own neutron irradiation results and available results in the literature. Details will not be repeated here but they reported that all the investigations into void swelling in molybdenum showed void swelling values of less than 3%. To quote from their conclusions "the saturation process appears to be controlled primarily by the processes related to superlattice formation".

In contrast with the above results, Brimhall and Simonen [14], who examined the variation of void parameters with displacement dose in molybdenum at 1000°C, found no indication of void swelling saturation. There appeared to be a close to linear relation between displacement damage and swelling even though void lattice formation had occurred at low doses. Ghoniem et al. [10] pointed out from this result that saturation does not necessarily occur when the void lattice is formed. However, this does not preclude its later

appearance and in the Ref. [14] results it is relevant that there are no swelling values above 3%. If the data is plotted in a linear-linear plot, Fig.1, the continued rise of swelling above ~2% depends entirely on the single 3% experimental point near 200 dpa. Thus these results are not inconsistent with saturation swelling. Certainly if the three papers on molybdenum above are considered together, the experimental evidence for a correlation between void swelling saturation (below ~3%) and void lattice formation appears soundly based. Particular support for this comes from the high swelling values found by Stubbins et al. [12] in the high temperature regime where no void lattice was found.

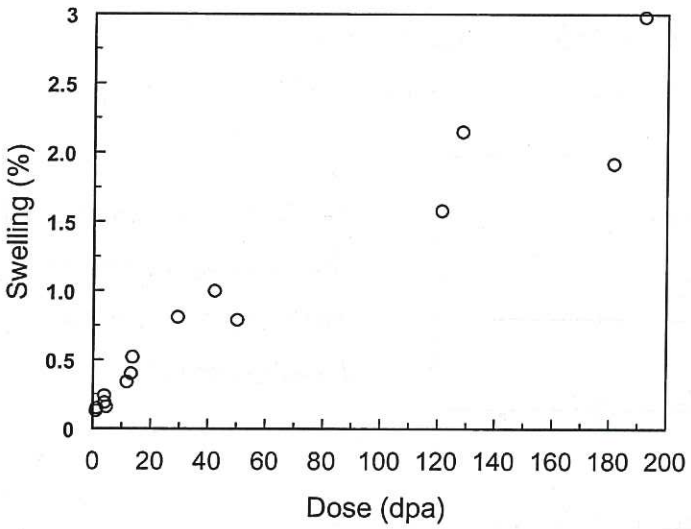

Fig.1. Data for void swelling against displacement damage in molybdenum at 1000°C, taken from fig.3 of Brimhall and Simonen [14] but redrawn in a linear plot

2.1.2. Tantalum

In tantalum void lattice formation has been reported by Wiffen [15] and by Loomis and Gerber [16] but the data is rather limited and insufficient to give any direct evidence for void swelling saturation. However, taken together it is interesting that in both sets of work where void lattice formation was found, the swelling is close to 2.5% even though the displacement damage values differ by more than a factor of two. In the Wiffen work the swelling value is quoted by the author but for the Loomis and Gerber results the swelling has been calculated by combining the quoted figures of void density and average void size. This is worth noting since the authors give two size parameters for the voids, one the average size as used above, the other the diameter, $d_{<100>}$, about 45% larger, obtained from a volume where the void lattice was as free of imperfections as possible.

2.1.3. Niobium

Loomis et al. [4] have produced detailed results on the response of niobium and Nb-1%Zr to ion irradiation damage, with over 40 data points relating the average void diameter and void lattice parameter to irradiation temperature over a wide range of damage from 20 to 120 displacements/atom (dpa). They found the results almost independent of damage, implying that void swelling saturation had already occurred before 20 dpa. This is shown clearly in Fig.2 below (fig.6 in ref [4]) where the $d_{<100>}$ void dimension (effectively the diameter, but see the comment for tantalum results above) is plotted as a function of displacement damage. After 20 dpa there is very little void growth. It is important to add that over the same dose range, the void lattice parameter remained constant, indicating that the void density was also constant: hence the saturation in swelling can be deduced.

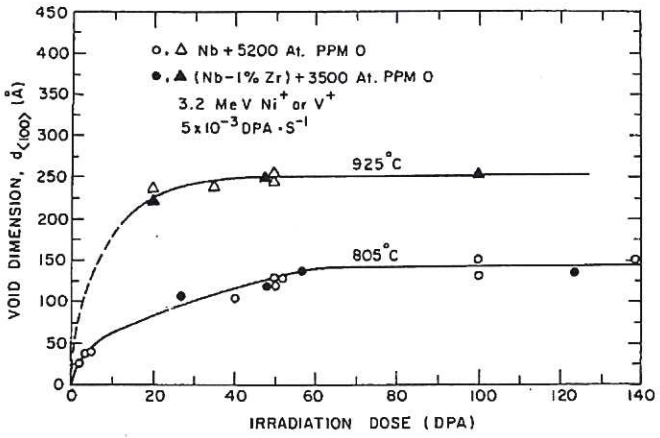

Fig.2. The variation of void size with dose in Nb and Nb1%Zr from the work of Loomis et al [4]

Although the indications of saturation swelling are clear, the swelling values deduced from the data in [4] shows that there is no fixed value for saturation swelling. This is seen here in Fig.3 where the swelling values are calculated using the data points from the plot given in [4] of void lattice spacing as a function of void dimension. In the simple calculation to derive the swelling values, the $d_{<100>}$ diameters were used and the bcc void lattice was assumed to be perfect. If the results of the same authors for tantalum regarding the mismatch between the $d_{<100>}$ and average diameter void values were carried over to niobium, the swelling could be grossly overestimated. This gives some difficulty in placing too much emphasis on the swelling values. However, even if there are quantitative doubts and a large scatter in the results, Fig.3 shows a clear increase of swelling with void lattice parameter (i.e. with drop in void density and increase in irradiation temperature).

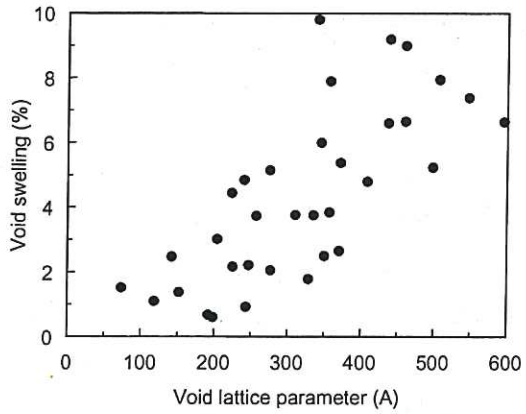

Fig.3. The variation of void swelling with void lattice parameter in ion irradiated niobium calculated from the data points in figure 10 of Loomis et al [4].

2.2 Fcc metals

2.2.1 Nickel

Kulcinski et al. [5] have found a seemingly perfect void lattice with an fcc structure in nickel after irradiation with selenium ions to a very high dose, 300 dpa. At the same time in this work they followed the void parameters carefully with dose and have produced convincing evidence of swelling saturation. This is reproduced below.

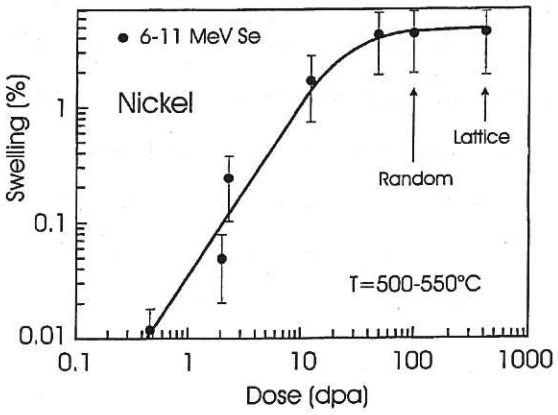

Fig. 3. A plot of swelling versus damage for nickel at 525°C [5]

Other investigations on pure nickel (but to lower doses) have not shown the above lattice formation. However, it is worth noting the work of Chen and Ardell [17] in which ion irradiation of Ni-Al alloys at 500°C for doses from 10 to 70 dpa showed that while no lattice formation was found in pure nickel samples, the phenomenon was seen clearly for alloys in the range 2 to 8 at.% Al. The best observations were in Ni-2Al, coinciding with the highest void concentration. The void swelling can be calculated easily from their void diameter and concentration figures. It varied between 6.7 and 7.7% for the pure nickel for doses of 20, 40 and 70 dpa, but significantly fell to between 1.05 and 2.0% for the Ni-2Al where the void

lattice was most clear. Possibly there is swelling saturation here for even the pure nickel but the most relevant point is that in no case was the swelling greater than 2% when void lattice formation was present.

2.2.2 Aluminium.

Evidence for void lattice formation in fcc metals is sparse. Besides the nickel example above, the only other metal for which void lattice formation has been reported is aluminium. This was first found by Mazey et al. [18] in material ion irradiated at 50 and 75°C to doses up to 80 dpa. The maximum swelling found was 3.2%. This compares with the value of 7.4% found at ~10 dpa in pure aluminium where no void lattice was observed [19].

A void lattice in aluminium was also found by Risbet and Levy in 1974 [20] under neutron irradiation but its rediscovery by Horsewell and Singh in 1987 [21] (again with neutrons) prompted the appellation 'hyperlattice' reflecting the large lattice parameter that could be deduced from the imperfect ordering. By drawing attention to the large intervoid distance Horsewell and Singh effectively ended any possibility that the void lattice formation might arise from void-void interaction; they concluded that 'long range defect transport must necessarily be anisotropic'.

The data in Ref. [21] is for a single dose (19 dpa) so no clear conclusion regarding saturation is possible. However, it is interesting that the swelling is of the order of only 2%, adding further to the idea that there might be a swelling limit associated with void lattice formation. It is worth noting that the 2% figure is not given by Horsewell and Singh but can be deduced by their 90nm average void diameter and the void concentration obtained from their f.c.c. void lattice spacing. It is important to recognise they made an error in equating the 200nm {100} lattice spacing to the void lattice parameter. Unfortunately this error has been promulgated by Golubov et al. [9] who deduced a value of 20% swelling based on the Horsewell-Singh lattice parameter.

3. Bubble lattice formation

There are many examples of bubble lattice formation in metals as a result of inert gas implantation [22]. It is worth commenting that although in the fcc, bcc and hcp metals the main geometrical features are identical as one moves from void lattices to bubble lattices, (strongly suggesting a common formation mechanism), there is no suggestion that there is any saturation swelling condition for bubbles. The review of Krishan [2] showed that the A/r parameter was significantly lower for bubble lattices, the implication being that the swelling was higher (much higher) than in void lattices. The simplest reason for this comes from the

different growth mechanisms for the two types of cavity, the void growth arising from the preferential acquisition of vacancies, the bubble growth coming from gas driven features. The implication is therefore that the swelling saturation in void lattices must be a feature arising from the growth mechanism.

4. Implications for void lattice models

4.1. Two-dimensional interstitial model

In discussing the implications of two dimensional SIA diffusion, Evans and Foreman [7] showed that the model leads to a maximum void radius given by

$$R_{max} = (2/\pi)[C^{-1} \exp(-4/Z_i)]^{1/3}$$

and therefore a maximum void swelling, S_{max}, given by

$$S_{max} = 1.08 \exp(-4/Z_i)$$

where C is the void concentration and Z_i the bias of dislocations for interstitials. The equations were derived very simply without for example considering any interactive sink strength terms or spatial effects. However, even if the equations above were refined, the straightforward picture would remain whereby the saturation arises from the different void sink strength response with size to the 2-d SIAs and the 3-d vacancies. Of particular relevance is that the maximum void swelling has values between 2 and 2.8% for Z_i between 1.0 and 1.1. This range is clearly close to the several experimental values found in this survey for different metals coincident with void lattice formation. The only results that provide some difficulty are those at higher temperatures in niobium. This has been explained previously [13] using the argument that although the model depends on the primary jumpstep being two-dimensional, the probability of rotational 3-d jumps must always exist. If this is so, any effects are more likely to be seen as the void spacing increases. In any case the probability may increase with temperature. How this will affect any saturation swelling value has not been calculated but one must expect it to increase rather than decrease the swelling.

4.2. One-dimensional interstitial diffusion

In the production bias model (PBM) for void swelling, small interstitial clusters formed in collision cascades glide large distances one-dimensionally. The saturation of void growth has been discussed in most detail by Golubov et al. [9]. It is shown that the swelling rate decreases with void size because of the increasing efficiency of the void in trapping the glissile SIA clusters and eventually vanishes when a maximum void size, R_v^{∞}, is reached;

hence there is a saturation in swelling. The main difference between the saturation for the 2-d SIA and 1-d SIA diffusion models is that in the latter case this saturation is for the void radius and not the void swelling. Although the value of R_v^∞ is a function of other parameters, d_{abs} and Z_v^d, the effective diameter of dislocations for absorbing dislocation loops and the efficiency of dislocations for trapping vacancies, respectively, there is no strong indication within the PBM that these parameters are particularly sensitive to temperature. Since any saturation swelling value will be dominated by the very large variations expected in void nucleation with temperature (Golubov et al. give excellent examples of this for Cu and Mo in their Fig.1), it strongly implies that there is no fixed value, or range of values, of the saturation swelling in the model. One must expect that if R_v^∞, is more or less constant, the associated swelling must decrease with increase in temperature as the void concentration falls. On this basis the predictions of any model based on single or multiple SIAs diffusing one-dimensionally is completely contrary to the behaviour of void swelling and void lattice formation in niobium discussed in section 2.1.3.

5. Conclusions

There appears to be sufficient experimental evidence in both bcc and fcc metals to conclude that there is a direct correlation between the presence of void lattices and a saturation in void swelling. As mentioned in this survey, this correlation has been deduced by several authors with the results on moybdenum, niobium and nickel being particularly important. Of interest are the large number of saturation swelling measurements around the 3% value. The data in niobium seems to provide the only exception though the actual swelling values has been questioned. While all models based on anisotropic SIA migration lead to saturation in either void radius or void swelling, the value of the swelling is consistent with the assumption that interstitials migrate two-dimensionally. One has to judge whether this agreement between experimental and theoretical saturation swelling could be coincidental. For models based on the one-dimensional diffusion of interstitials or interstitial clusters, it is difficult to see how a saturation of void radius could lead to the observed small range of swelling values associated with void lattice formation, or to the qualitative increase of saturation swelling with temperature seen in the niobium results. Whether any other model of void lattice formation could fit the experimental results is an open question.

This work was funded jointly by the United Kingdom Engineering and Physical Sciences Research Council and by EURATOM.

References

1. R. Bullough and R.C. Perrin, Theory of void formation and growth in irradiated metals, Albany Conf. on Radiation-Induced Voids in Metals, 1972, p.769; K. Malen and R. Bullough, Proc. Conf. on Voids Formed by Irradiation of Reactor Materials (eds. S.F. Pugh, M.H. Loretto and D.I.R. Norris), BNES, March 1971, p109.

2. K. Krishan, Ordering of voids and gas bubbles in radiation environments. Radiation Effects 66 (1982) 121-155.

3. G.L. Kulcinski, J.L. Brimhall and H.E. Kissinger, Production of voids in pure metals by high energy heavy-ion bombardment, Albany Conf. on Radiation-Induced Voids in Metals, 1972, p.449.

4. B.A. Loomis, S.E. Gerber and A. Taylor, Void ordering in ion irradiated niobium and Nb-1%Zr, J. Nucl. Mater. 68 (1977) 19.

5. G.L. Kulcinski, J.L. Brimhall and H.E. Kissinger, Production of voids in nickel with high energy selenium ions, J. Nucl. Mater. 40 (1971) 166.

6. J.H. Evans, Void and bubble lattice formation in molybdenum: a mechanism based on two dimensional self-interstitial diffusion, J. Nucl. Mater. 119 (1983) 180. See also: Irradiation-induced cavity lattice formation in metals, Patterns, Defects and Materials Instabilities, (eds. D. Walgraef and N.M. Ghoniem) Kluwer Acad. Publishers, 1990, p. 347.

7. J.H. Evans and A.J.E. Foreman, Some implications of anisotropic self-interstitial diffusion on void swelling in metals, J. Nucl. Mater. 137 (1985) 1.

8. H. Trinkaus, B.N. Singh and A.J.E Foreman, Glide of interstitial loops produced under cascade damage conditions: possible effects on void formation, J. Nucl. Mater. 199 (1992) 1.

9. S.I. Golubov, B.N. Singh and H. Trinkaus, Defect accumulation in fcc and bcc metals and alloys under cascade conditions, J. Nucl. Mater. 276 (2000) 78.

10. N.M. Ghoniem, D. Walgraef and S.J. Zinkle, Theory and experiment of nanostructure self-organisation in irradiated metals, J. Computer-Aided Materials Design 8 (2002) 1.

11. H.L. Heinisch and B.N. Singh, The effects of one-dimensional migration of self-interstitial clusters on the formation of void lattices, J. Nucl. Mater. 307 (2002) 876.

12. J.F. Stubbins, J. Moteff and A.Taylor, Void swelling in V+ ion irradiated Mo, J. Nucl. Mater. 101 (1981) 64.

13. F.A. Garner and J.F. Stubbins, Saturation of swelling in neutron irradiated molybdenum, J. Nucl. Mater. 212-215 (1994) 1298.

14. J.L. Brimhall and E.P. Simonen, Void swelling in ion-bombarded molybdenum, J. Nucl. Mater. 52 (1974) 323.

15. F.W. Wiffen, The microstructure and swelling of neutron irradiated tantalum, J. Nucl. Mater. 67 (1977) 119.

16. B.A. Loomis and S.B. Gerber, Ordered void arrays in ion irradiated Ta, J. Nucl. Mater. 71 (1978) 377.

17. L.J. Chen and A.J. Ardell, Void ordering in nitrogen-ion irradiated nickel aluminium solid solutions, J. Nucl. Mater. 75 (1978) 177.

18. D.J. Mazey, S. Francis and J.A. Hudson, Observation of a partial ordered void lattice in aluminium irradiated with 400 keV Al+ ions, J. Nucl. Mater. 47 (1973) 137.

19. N.H. Packan, Fluence and flux dependence of void formation in pure aluminum, J. Nucl. Mater. 40 (1971) 1.

20. A Risbet and V. Levy, J. Nucl. Mater. 50 (1974) 116.

21. A. Horsewell and B.N. Singh, Void hyperlattices in high purity aluminium irradiated with fast neutrons, Rad. Effects 102 (1987) 1.

22. P.B. Johnson, D.J. Mazey and J.H. Evans, Bubble structures in helium irradiated metals, Rad. Effects 78 (1983) 147.